

Multipartite Dense Coding vs. Quantum Correlation: Noise Inverts Relative Capability of Information Transfer

Tamoghna Das, R. Prabhu, Aditi Sen(De), and Ujjwal Sen
Harish-Chandra Research Institute, Chhatnag Road, Jhansi, Allahabad 211 019, India

A highly entangled bipartite quantum state is more advantageous for the quantum dense coding protocol than states with low entanglement. Such a correspondence, however, does not exist even for pure quantum states in the multipartite domain. We establish a connection between the multipartite capacity of classical information transmission in quantum dense coding and several multipartite quantum correlation measures of the shared state, used in the dense coding protocol. In particular, we show that for the noiseless channel, if multipartite quantum correlations of an arbitrary multipartite state of arbitrary number of qubits is the same as that of the corresponding generalized Greenberger-Horne-Zeilinger state, then the multipartite dense coding capability of former is the same or better than that of the generalized Greenberger-Horne-Zeilinger state. Interestingly, in a noisy channel scenario, where we consider both uncorrelated and correlated noise models, the relative abilities of the quantum channels to transfer classical information can get inverted by administering a sufficient amount of noise. When the shared state is an arbitrary multipartite mixed state, we also establish a link between the classical capacity for the noiseless case and multipartite quantum correlation measures.

I. INTRODUCTION

In recent times, a lot of interest has been created to characterize and quantify quantum correlations in multipartite quantum systems [1–4]. This is due to the fact that the preparation of multiparticle states with quantum coherence enables us to realize several quantum information protocols like quantum dense coding [5], quantum teleportation [6], secure quantum cryptography [7], and one way quantum computation [8], in a way that is better than their classical counterparts. This increasing interest is further boosted by the latest advances in experiments to realize multipartite states in different physical systems including photons, ion traps, optical lattices, and nuclear magnetic resonances [9–14].

It has been shown, both theoretically as well as experimentally, that bipartite entanglement is an essential ingredient for a vast majority of known quantum communication schemes, involving two parties. Specifically, it has been established that in the case of pure bipartite states, the capacity of classical information transmission via quantum states increases with the increase of any quantum correlation measure. Such a simple scenario is facilitated by the fact that quantum correlation in a bipartite pure quantum state, in the asymptotic domain, can be *uniquely* quantified by the local von Neumann entropy [1]. The situation is far richer in the multipartite case (see Refs. [15–24]). Regarding the entanglement content, in a multipartite quantum state, which ranges from being bipartite to genuine multipartite, even multipartite *pure* states can be classified in several ways [25] and therefore, there is no unique measure that can determine quantum correlations, present in the system.

Unlike point to point communication, where among two parties, one acts as a sender and the other as a receiver, communication protocols involving multiple parties can have various complexities. One possible scenario

involves several senders and a single receiver. Suitable examples for such multipartite communication protocols include, when several news reporters from different locations send various news articles to the newspaper editorial office or when several weather observers from different places communicate their respective weather reports to the regional meteorological office.

In this paper, we connect multipartite communication protocols with multipartite quantum correlation measures. In particular, we establish a relation between the capacity of multipartite dense coding and multipartite quantum correlation measures of arbitrary multiqubit states. This correspondence is illustrated both in the case of noiseless and noisy channels for arbitrary shared states. Specifically, we show that in the case of the noiseless quantum channel, if the capacity of classical information transmission using the generalized Greenberger-Horne-Zeilinger (g GHZ) state [26] is the same as that of any multiqubit pure state, then the multipartite quantum correlation of the g GHZ state is either the same or higher than that of the latter states. The result is generic in the sense that it does not rely on the choice of the quantum correlation measure, and is independent of the number of parties. Three computable measures, the generalized geometric measure [24, 27, 28], the tangle [29] and discord monogamy score [30, 31], are considered for obtaining the results. It is to be noted that while the first multipartite measure is based on the geometry of the space of multipartite quantum states, the latter two are based on the concept of monogamy of quantum correlations.

The noisy case can be considered at several levels of complexity. Here we consider the following two situations. First, we consider the case when the noise is present before the encoding of classical information, while the quantum channel that transmits the encoded state is noiseless. Secondly, we consider the situation when the encoding is performed on a pure shared state, while the post-encoded state is sent via a noisy quan-

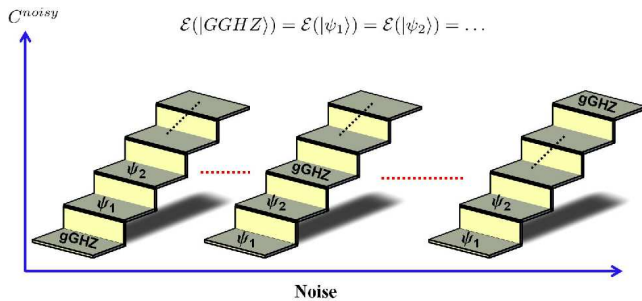


FIG. 1. Schematic diagram of the change of status of the g GHZ state in comparison to other multipartite states with respect to multipartite DC capacity in the presence of noise. The comparison has been made with the states which possess the same amount of multipartite quantum correlations as the g GHZ state. The results obtained in this paper show that the g GHZ state is more robust against noise as compared to arbitrary states for the dense coding protocol. This is independent of the fact whether the noise in the system is from the source or in the channel after the encoding.

tum channel. In the first case, we begin by obtaining a sufficient condition for dense codeability for arbitrary, possibly mixed, multipartite quantum states. We perform numerical simulations by generating Haar uniform rank-2 three-qubit states, and find that a great majority of them are better carriers of classical information than the g GHZ state with the same multiparty quantum correlation content. Numerical analysis of higher-rank states are also considered.

Going over to the second case, when the quantum channel is noisy, we show that the presence of noise can invert the relative capability of information transfer for two states with the same multiparty quantum correlation content. In particular, we find that the effect of both correlated and uncorrelated covariant noise with respect to the capability of classical information transfer is less pronounced on the g GHZ state as compared to a generic pure multiparty state. This relative suppression of the effect of noise for the g GHZ state is what results in the inversion of the relative capabilities of information transfer between a g GHZ state and a generic pure multiparty quantum state. A schematic diagram elucidating the situation is presented in Fig. 1.

The paper is organized as follows. In Sec. II, we describe the quantum correlation measures that are used later in the paper. In the subsequent section (Sec. III), we discuss the capacities of the quantum dense coding protocol, with and without noise. In Sec. IV, we establish the connection between the capacity and the quantum correlation measures for the noiseless channel, while we deal with the noisy channels in Sec. V. In particular, we deal with the fully correlated Pauli channel in Sec. VA and with the uncorrelated Pauli channel in Sec. VB. We present a conclusion in Sec. VI.

II. QUANTUM CORRELATION MEASURES

Quantum correlations present in bipartite quantum systems can broadly be classified into two paradigms – (a) entanglement-separability and (b) information-theoretic. Measures of the former paradigm always vanish for separable states. Examples include entanglement of formation [32], concurrence [33], distillable entanglement [32], and logarithmic negativity [34]. On the other hand, information-theoretic quantum correlation measures are independent of entanglement, and examples include quantum discord [35] and quantum work deficit [36]. In the present section, we define concurrence and quantum discord, and then discuss monogamy relations based on these two measures. Finally we define a multipartite entanglement measure, the generalized geometric measure, based on the concept of the Fubini-study metric [24, 27] (cf. [28]).

A. Concurrence

Concurrence is a quantum correlation measure for two-qubit systems, which is a monotonic function of entanglement of formation [33]. For an arbitrary two-qubit state, ρ_{AB} , it is given by

$$\mathcal{C}(\rho_{AB}) = \max\{0, \lambda_1 - \lambda_2 - \lambda_3 - \lambda_4\}, \quad (1)$$

where the λ_i 's are the square roots of the eigenvalues of $\rho_{AB}\tilde{\rho}_{AB}$ in decreasing order and $\tilde{\rho}_{AB} = (\sigma_y \otimes \sigma_y)\rho_{AB}^*(\sigma_y \otimes \sigma_y)$, with the complex conjugate being taken in the computational basis. Concurrence vanishes for all separable states while it is maximal for any maximally entangled state.

B. Quantum Discord

Quantum discord is an information-theoretic quantum correlation measure, which is obtained by taking the difference between two inequivalent forms of quantum mutual information. Mutual information quantifies the correlation between two systems. Classically, it can be defined in two equivalent ways. For two variables, X and Y , it is defined as

$$I(X, Y) = H(X) + H(Y) - H(X, Y), \quad (2)$$

where $H(X) = -\sum_x p_x \log_2 p_x$ is the Shannon entropy, with p_x being the probability of x occurring as a value for the classical variable X , and similarly for $H(Y)$. $H(X, Y)$ denotes the Shannon entropy of the joint probability distribution of X and Y . Using Bayes' rule, one can rewrite the mutual information in terms of conditional entropy, $H(X|Y)$, to obtain

$$I(X, Y) = H(X) - H(X|Y). \quad (3)$$

In the quantum domain, these two classically equivalent definitions of mutual information become unequal and their difference has been proposed to be a measure of quantum correlation, called the quantum discord [35, 37]. For any composite system, ρ_{AB} , quantizing the first definition of the mutual information, one obtains

$$\mathcal{I}(\rho_{AB}) = S(\rho_A) + S(\rho_B) - S(\rho_{AB}), \quad (4)$$

where $S(\varrho) = -\text{Tr}(\varrho \log \varrho)$ is the von Neumann entropy of ϱ . This quantity has been argued to be total correlation in the bipartite state [35]. Quantizing the second definition is not straightforward, since the quantity obtained by replacing the Shannon entropies by the von Neumann ones can be negative for some quantum states [38]. To overcome this drawback, one can make a measurement on one of the subsystems, say subsystem B , of ρ_{AB} , and the measured conditional entropy of ρ_{AB} can be obtained as

$$S(\rho_{A|B}) = \min_{\{B_i\}} \sum_i p_i S(\rho_{A|i}), \quad (5)$$

where the rank-1 projection-valued measurement $\{B_i\}$ is performed on the B -part of the system. Here $\rho_{A|i} = (1/p_i)(\text{Tr}_B[(\mathbb{1}_A \otimes B_i)\rho_{AB}(\mathbb{1}_A \otimes B_i)])$, with $p_i = \text{Tr}_{AB}[(\mathbb{1}_A \otimes B_i)\rho_{AB}(\mathbb{1}_A \otimes B_i)]$, and $\mathbb{1}_A$ being the identity operator on the Hilbert space of subsystem A . Using this quantity, one then quantizes the second definition of mutual information as

$$\mathcal{J}(\rho_{AB}) = S(\rho_A) - S(\rho_{A|B}), \quad (6)$$

which has been argued to be a measure of classical correlation of the bipartite state [35]. Finally, the quantum discord is defined as

$$\mathcal{D}(\rho_{AB}) = \mathcal{I}(\rho_{AB}) - \mathcal{J}(\rho_{AB}). \quad (7)$$

C. Monogamy score: Tangle and Discord Monogamy Score

Monogamy of quantum correlations quantifies the sharability of the same in multipartite systems [29]. For an arbitrary $(N+1)$ -party quantum state, $\rho_{A_1 A_2 \dots A_N B}$, let $\mathcal{Q}_{A_i B}$ ($i = 2, \dots, N$) be the amount of a certain quantum correlation shared between the pair $A_i B$ ($i = 2, \dots, N$), and $\mathcal{Q}_{A_1 A_2 \dots A_N : B}$ represent the same between B and rest of the parties. Here B acts as a ‘‘nodal’’ observer. The state $\rho_{A_1 A_2 \dots A_N B}$ is said to be monogamous for the quantum correlation measure, \mathcal{Q} , if [29]

$$\sum_{i=1}^N \mathcal{Q}_{A_i B} \leq \mathcal{Q}_{A_1 A_2 \dots A_N : B}. \quad (8)$$

Using the terms of the above relation, we define the monogamy score for the quantum correlation measure, \mathcal{Q} , as

$$\delta_{\mathcal{Q}} = \mathcal{Q}_{A_1 A_2 \dots A_N : B} - \sum_{i=1}^N \mathcal{Q}_{A_i B}, \quad (9)$$

for B as the nodal observer. Therefore, \mathcal{Q} is monogamous for a given state when $\delta_{\mathcal{Q}}$ is positive for that state. Otherwise, the measure is said to be non-monogamous for that state. The advantage of such a multipartite quantum correlation measure is that it can be expressed in terms of bipartite quantum correlation measures.

In Eq. (9), if \mathcal{Q} is chosen to be the square of the concurrence, then we obtain the tangle [29], which is known to be monogamous for all multiqubit states [29, 39]. Choosing \mathcal{Q} to be quantum discord, we obtain the discord monogamy score [31], which can be negative even for some three qubit pure states [30].

D. Generalized Geometric Measure

Let us now define a genuine multipartite entanglement measure. An N -party pure state is said to be genuinely multipartite entangled if it is non-separable with respect to every bipartition. The generalized geometric measure (GGM) is obtained by considering the minimal distance from the set of all multipartite states that are not genuinely multipartite entangled [24, 27] (cf. [28]). More specifically, the GGM of an N -party pure quantum state $|\phi_N\rangle$ is defined as

$$\mathcal{E}(|\phi_N\rangle) = 1 - \Lambda_{\max}^2(|\phi_N\rangle), \quad (10)$$

where $\Lambda_{\max}(|\phi_N\rangle) = \max |\langle \chi | \phi_N \rangle|$, with the maximization being taken over all pure states $|\chi\rangle$ that are not genuinely N -party entangled. It was shown in Ref. [24, 27] that $\mathcal{E}(|\phi_N\rangle)$ reduces to

$$\mathcal{E}(|\phi_N\rangle) = 1 - \max \{ \lambda_{\mathcal{A}:\mathcal{B}}^2 | \mathcal{A} \cup \mathcal{B} = \{1, 2, \dots, N\}, \mathcal{A} \cap \mathcal{B} = \emptyset \}, \quad (11)$$

where $\lambda_{\mathcal{A}:\mathcal{B}}$ is the maximal Schmidt coefficients in the $\mathcal{A} : \mathcal{B}$ bipartite split of $|\phi_N\rangle$.

III. QUANTUM DENSE CODING

In this section, we define the capacities of dense coding, when an arbitrary multipartite state is used as a channel, shared between several senders and a single receiver. We first consider the scenario of a noiseless channel and then derive the capacity for a noisy covariant channel.

A. Quantum dense coding via noiseless channel

The capacity of the quantum dense coding protocol quantifies the amount of classical information that can be transferred via a quantum state used as a channel, when an additional quantum channel, which may be noiseless or noisy, is also available. We begin with the noiseless case. For an arbitrary two-party state, ρ_{SR} , shared between the sender, S , and the receiver, R , the capacity of

dense coding (DC) of ρ_{SR} is given by [21, 40, 41]

$$C(\rho_{SR}) = \frac{1}{\log_2 d_{SR}} \max\{\log_2 d_S, \log_2 d_S + S(\rho_R) - S(\rho_{SR})\}, \quad (12)$$

where d_S is the dimension of the Hilbert space on which the senders' part of the state ρ_{SR} is defined, and where d_{SR} is that on which the entire state ρ_{SR} is defined. Here, ρ_R is local density matrix of the receiver's part. The denominator, $\log_2 d_{SR}$, is incorporated to make the capacity dimensionless. Note that we are considering the case of unitary encoding (for non-unitary encoding, see [42, 43]), and where the additional quantum channel is noiseless. The noisy case is considered below. When $S(\rho_R) - S(\rho_{SR}) > 0$, a shared quantum state is better for classical information transmission than any classical protocol with the same resources. It immediately implies that any bipartite pure entangled state is a good quantum channel for dense coding.

In the multipartite regime, let us consider the scenario where there are N senders, S_1, \dots, S_N and a single receiver, R . For the quantum state, $\rho_{S_1 \dots S_N R}$, shared between the $N+1$ parties, the capacity of DC with unitary encoding and for noiseless additional quantum channel is given by [21, 41]

$$C(\rho_{S_1 \dots S_N R}) = \frac{1}{\log_2 d_{S_1 \dots S_N R}} \max\{\log_2 d_{S_1 \dots S_N}, \log_2 d_{S_1 \dots S_N} + S(\rho_R) - S(\rho_{S_1 \dots S_N R})\}, \quad (13)$$

where $d_{S_1 \dots S_N} = d_{S_1} \dots d_{S_N}$, with d_{S_1}, \dots, d_{S_N} being the dimensions of the Hilbert spaces corresponding to the individual senders, and $d_{S_1 \dots S_N R}$ is the total dimension of the Hilbert space on which the entire multipartite state is defined. The state is therefore dense codeable if $S(\rho_R) - S(\rho_{S_1 \dots S_N R}) > 0$. In this paper, whenever we call a multipartite state as dense codeable, it implies that the state is good for dense coding with multiple senders and a single receiver.

B. Capacity of quantum dense coding through noisy channel

Consider now the situation of classical information transmission when the additional quantum channel is noisy. We assume that after local unitary encoding, the particles are sent through a noisy quantum channel. We consider here a particular class of channels, known as the covariant channels, denoted by Λ . Such a channel is a completely positive map with the property that it commutes with a complete set of orthogonal unitary operators, $\{W_i\}$, i.e.,

$$\Lambda(W_i \rho W_i^\dagger) = W_i \Lambda(\rho) W_i^\dagger, \quad \forall i. \quad (14)$$

The multipartite dense coding capacity has already been calculated for this channel [43] and is given by

$$C^{noisy}(\rho_{S_1 \dots S_N R}) = \frac{1}{\log_2 d_{S_1 \dots S_N R}} \max\{\log_2 d_{S_1 \dots S_N}, \log_2 d_{S_1 \dots S_N} + S(\rho_R) - S(\tilde{\rho})\}, \quad (15)$$

where

$$\tilde{\rho} = \Lambda \left((U_{S_1 S_2 \dots S_N}^{min} \otimes I_R) \rho_{S_1 \dots S_N R} (U_{S_1 S_2 \dots S_N}^{min \dagger} \otimes I_R) \right).$$

Here, $U_{S_1 S_2 \dots S_N}^{min}$ denotes the unitary operator on the senders' side, which minimizes the von Neumann entropy of $(U_{S_1 \dots S_N} \otimes I_R) \rho_{S_1 \dots S_N R} (U_{S_1 \dots S_N}^\dagger \otimes I_R)$ over the set of unitaries $\{U_{S_1 S_2 \dots S_N}\}$, that can be global as well as local. It is reasonable from a practical point of view to assume that the senders perform local encoding. Then $U_{S_1 S_2 \dots S_N}^{min}$ will have the form given by

$$U_{S_1 S_2 \dots S_N}^{min} = U_{S_1}^{min} \otimes U_{S_2}^{min} \otimes \dots \otimes U_{S_N}^{min}. \quad (16)$$

Since only the particles of the senders are sent through the noisy channel (after the unitary encoding), the entropy of the receiver's side remains unchanged. Depending on the structure of Λ , the channel can be either correlated or uncorrelated.

In Eqs. (12), (13) and (15), for convenience, we call the second terms within the maximum in the numerators, divided by the denominators, as the corresponding "raw" capacities. We use the same notation for the raw capacity as the corresponding original capacity, but the context will always make the choice clear.

Pauli Channel

The Pauli channel is an example of a covariant channel. When an arbitrary two-dimensional quantum state is sent through the Pauli channel, the state is rotated by any one of the Pauli matrices, $\sigma_x, \sigma_y, \sigma_z$, or left unchanged. If the σ_x, σ_y , and σ_z act respectively with the probabilities λ_x, λ_y , and λ_z , then the transformed state is

$$\rho' = \lambda_x \sigma_x \rho \sigma_x + \lambda_y \sigma_y \rho \sigma_y + \lambda_z \sigma_z \rho \sigma_z + (1 - \lambda_x - \lambda_y - \lambda_z) \rho. \quad (17)$$

For $\lambda_x = \lambda_y = \lambda_z = p/3$, the channel represents the depolarizing channel [44].

IV. RELATIONSHIP BETWEEN MULTIPARTY QUANTUM CORRELATIONS AND DENSE CODING CAPACITY: NOISELESS CHANNEL

In this section, we establish a generic relation between the capacity of dense coding and various quantum correlation measures, defined in Sec. II. The analytical results obtained in this section are for quantum systems with $(N+1)$ -qubits, consisting of N senders and a single

receiver. The numerical simulations that are performed to visualize the results are for three-qubit pure as well as mixed states. Throughout this section, we consider the case when the additional quantum channel, that is used post-encoding, is noiseless.

A. Connection between Capacity and Multipartite Quantum Correlations for Pure States

In a bipartite scenario, all the pure states with the same amount of entanglement have equal capacity of dense coding. The entanglement in this case is uniquely classified by the von Neumann entropy of the local density matrices and the capacity is maximal for the maximally entangled states.

We will see that this simple situation is no more true in the multipartite regime. However, it is still possible to obtain a generic relation between capacity and entanglement. In a multipartite scenario, quantification of quantum correlations is not unique even for pure states and hence each measure, in principle, identifies its own distinct state with maximal quantum correlation. Nevertheless, the Greenberger-Horne-Zeilinger (GHZ) state [26] has been found to possess a high amount of multipartite quantum correlation, according to violation of certain Bell inequalities [45], as well as according to several multipartite entanglement measures [24, 27, 28]. In view of these results, we compare the properties of an arbitrary $(N+1)$ -qubit pure state with that of the $(N+1)$ -qubit generalized GHZ state ($gGHZ$), which is given by

$$|gGHZ\rangle_{S_1 S_2 \dots S_N R} = \sqrt{\alpha} |0_{S_1} \dots 0_{S_N}\rangle |0_R\rangle + \sqrt{1-\alpha} e^{i\phi} |1_{S_1} \dots 1_{S_N}\rangle |1_R\rangle, \quad (18)$$

where α is the real number in $(0,1)$ and $\phi \in [0, 2\pi)$. We find that if the capacity of dense coding of an arbitrary $(N+1)$ -party state, $|\psi\rangle$, and the $gGHZ$ state are the same, then the quantum correlations of these two states may not be the same. However, they follow an ordering, which we establish in the following two theorems. The feature is generic in the sense that it holds for drastically different choices of the quantum correlation measures. Here on, we skip all the subscripts in the notation of the states, for simplicity.

Theorem 1: *Of all the multiqubit pure states with an arbitrary but fixed multipartite dense coding capacity, the generalized GHZ state has the highest GGM.*

Proof. Scanning over α in Eq. (18), one can obtain an arbitrary value of the GGM. Therefore to prove the theorem, one needs to show that if the multipartite dense coding capacity of an arbitrary $(N+1)$ -qubit pure state is the same as that of an $(N+1)$ -party $gGHZ$ state, then the genuine multipartite entanglement, as quantified by the GGM, of that arbitrary pure state is bounded above by that of the $gGHZ$ state, i.e.,

$$\mathcal{E}(|\psi\rangle) \leq \mathcal{E}(|gGHZ\rangle). \quad (19)$$

The multipartite dense coding capacities of the $(N+1)$ -party $gGHZ$ state and the arbitrary pure state, $|\psi\rangle$, can be obtained by using Eq. (13), and are given respectively by

$$C(|gGHZ\rangle) = \frac{N}{N+1} - \frac{\alpha \log_2 \alpha + (1-\alpha) \log_2 (1-\alpha)}{N+1}$$

and

$$C(|\psi\rangle) = \frac{N}{N+1} - \frac{\lambda_R \log_2 \lambda_R + (1-\lambda_R) \log_2 (1-\lambda_R)}{N+1},$$

where λ_R is the maximum eigenvalue of the marginal density matrix, ρ_R , of the receiver's part of the state $|\psi\rangle$. The GGMs for the $gGHZ$ state and the $|\psi\rangle$ are obtained respectively by

$$\mathcal{E}(|gGHZ\rangle) = 1 - \alpha, \quad (20)$$

$$\mathcal{E}(|\psi\rangle) = 1 - \max\{\{l_A\}\}, \quad (21)$$

where we assume that $\alpha \geq \frac{1}{2}$. The set $\{l_A\}$ contains the maximum eigenvalues of the reduced density matrices of all possible bipartitions of $|\psi\rangle$. Equating the multipartite dense coding capacities for these two states, we obtain

$$\alpha = \lambda_R. \quad (22)$$

Note that $\lambda_R \in \{l_A\}$. Let us now consider the two following cases: (1) the maximum in GGM is attained by λ_R , and (2) the maximum is attained by an eigenvalue which is different from λ_R .

Case 1: Suppose $\lambda_R = \max\{\{l_A\}\}$. Then

$$\mathcal{E}(|\psi\rangle) = 1 - \lambda_R = 1 - \alpha = \mathcal{E}(|gGHZ\rangle), \quad (23)$$

by using Eq. (22).

Case 2: Suppose $\lambda_R \neq \max\{\{l_A\}\}$. Let $\lambda_R \leq \lambda_0 = \max\{\{l_A\}\}$. Therefore, we obtain

$$\mathcal{E}(|\psi\rangle) = 1 - \lambda_0 \leq 1 - \lambda_R = 1 - \alpha = \mathcal{E}(|gGHZ\rangle)$$

Hence the proof. \blacksquare

We randomly generate 10^5 arbitrary three-qubit pure states by using the uniform Haar measure on this space and plot the behavior of the GGM versus the DC capacity for these states. As proven in Theorem 1, the scatter diagram populates only a region outside the parabolic curve of the $gGHZ$ states. See Fig. 2. Interestingly, therefore, in the plane of the dense coding capacity and the GGM, there exists a forbidden region which cannot be accessed by any three-qubit pure state. With respect to dense coding in the noiseless case, therefore, the $gGHZ$ state is the least useful state among all states having an equal amount of the multipartite entanglement.

We now show that the result is potentially independent of the choice of the multipartite quantum correlation measure. Towards this aim, let us now consider the tangle and the discord monogamy score, as multipartite quantum correlation measures. The relations between

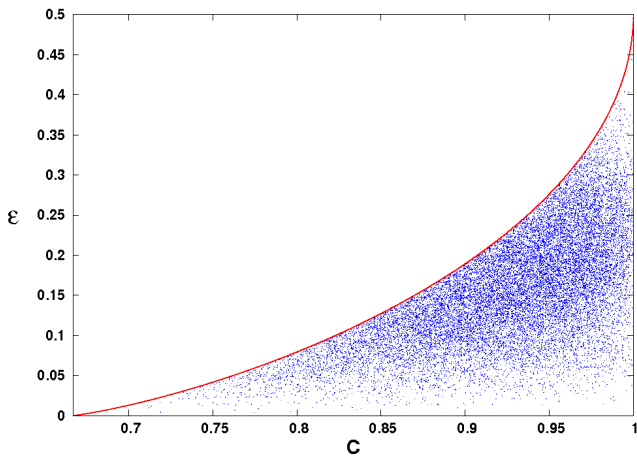


FIG. 2. (Color online.) GGM vs. multipartite DC capacity. GGM is plotted as the ordinate while multipartite DC capacity is plotted as the abscissa for 10^5 randomly chosen three-qubit pure states, according to the uniform Haar measure over the corresponding space (blue dots). The red line represents the generalized GHZ states. There is a set of states for which, if the capacity matches with a g GHZ state, then their GGMs are also equal. For the remaining states, if the capacity is equal to a g GHZ state, its GGM is bounded above by that of the g GHZ state. Note that the range of the horizontal axis is considered only when the states are dense codeable. The quantities represented on both the axes are dimensionless. We are considering the case where the post-encoded states are sent through noiseless channels.

these two quantum correlation measures and the capacity of DC are established in the following theorem.

Theorem 2: *Of all multiqubit pure states with an arbitrary but fixed multipartite dense coding capacity, the generalized GHZ state has the highest tangle as well as the highest discord monogamy score.*

Note: The tangle and discord monogamy score are defined here by using the receiver of the DC protocol as the nodal observer.

Proof. The equality of the multipartite dense coding capacities of the $(N+1)$ -party g GHZ state and the arbitrary pure state, $|\psi\rangle$, implies that $\alpha = \lambda_R \geq 1/2$. Notations are the same as in the proof of Theorem 1. Note that the tangle of the g GHZ state is $4\alpha(1-\alpha)$. Therefore, we have

$$\begin{aligned} \delta_{\mathcal{C}^2}(|\psi\rangle) &= 4\lambda_R(1-\lambda_R) - \sum_i \mathcal{C}^2(\rho_{S_i R}) \\ &\leq 4\lambda_R(1-\lambda_R) = 4\alpha(1-\alpha) = \delta_{\mathcal{C}^2}(|gGHZ\rangle). \end{aligned} \quad (24)$$

The inequality in the second line is due to the fact that $\mathcal{C}^2(\rho_{S_i R})$ are non-negative, where $\rho_{S_i R}$ is the density matrix of the sender S_i and the receiver R corresponding to

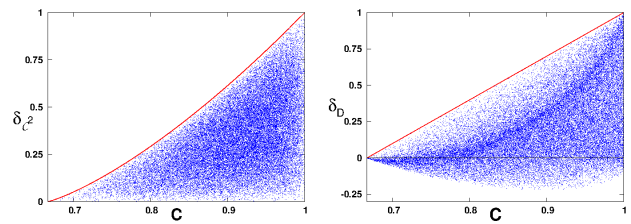


FIG. 3. (Color online.) Left: Tangle (vertical axis) vs. multipartite DC capacity (horizontal axis) for randomly generated three-qubit pure states (blue dots). Right: Discord monogamy score (vertical axis) vs. DC capacity (horizontal axis) for the same states. In both the cases, the g GHZ states give the boundary (red line). The capacity is dimensionless, while the tangle and discord monogamy score are measured in ebits and bits, respectively. All other considerations are the same as in Fig. 2.

the state $|\psi\rangle$. Similarly, for the discord score, we have

$$\begin{aligned} \delta_{\mathcal{D}}(|\psi\rangle) &= S(\rho_R) - \sum_i \mathcal{D}(\rho_{S_i R}) \\ &\leq S(\rho_R) = S(\alpha) = \delta_{\mathcal{D}}(|gGHZ\rangle), \end{aligned} \quad (25)$$

since $0 \leq \mathcal{D}(\rho_{S_i R}) \leq 1$. Here, $S(\alpha)$ denotes the von Neumann entropy of the single-side density matrix of the g GHZ state. Hence the proof. ■

To visualize the above theorem, we randomly generate 10^5 pure three-qubit states, by using the uniform Haar measure in the corresponding space, and prepare scatter diagrams for tangle versus the multipartite DC capacity (Fig. 3 (left)) and for the discord monogamy score versus the same capacity (Fig. 3 (right)). The simulations are clearly in agreement with Theorem 2. In particular, and just like for GGM versus the capacity, the planes of $(C, \delta_{\mathcal{C}^2})$ and $(C, \delta_{\mathcal{D}})$ can not be fully accessed by the three-qubit pure states.

B. Capacity vs. Multipartite Quantum Correlations for Shared Mixed States

We now investigate the relation between DC capacity and multipartite quantum correlation measures, when the shared state is an arbitrary $(N+1)$ -party mixed state. In this case, to establish such connection, the main difficulty is that there are only a few quantum correlation measures available which can be computed. In this case, therefore, we consider the discord monogamy score as the multipartite quantum correlation measure, since quantum discord can be numerically calculated for arbitrary bipartite systems, and investigate its connection with the DC capacity.

In Fig. 4, we randomly generate 10^5 mixed states of rank-2 in the space of three-qubit states and plot the discord monogamy score with respect to the DC capacity. The random generation is with respect to the uniform Haar measure induced from that in the appropriate

higher-dimensional pure state space. The numerical simulation reveals that Theorem 2 does not hold for rank-2 (mixed) three-qubit states. In particular, we find that if a g GHZ state and a rank-2 three-qubit mixed state have the same discord monogamy score, then sharing the g GHZ state is usually more beneficial than the mixed state, for performing the multipartite DC protocol. More precisely, among randomly generated 10^5 rank-2 states, there are only 1.85% states which satisfy Theorem 2. We will later show that a similar picture is true for the noisy channel. This implies that in the presence of noisy environments, irrespective of whether the noise is afflicted before or after encoding, it is typically better to share a g GHZ state among states with a given discord monogamy score, from the perspective of DC capacity. Before presenting the results obtained by using numerical simulations for higher-rank mixed states, let us discuss the behavior of the DC capacity, as enunciated in the following proposition. We will find that it can be used to intuitively understand the numerical results for higher-rank states presented below.

Proposition 1: *An arbitrary $(N + 1)$ -qubit (pure or mixed) state is dense codeable if the maximum eigenvalue of the $(N + 1)$ -party state is strictly greater than the maximum eigenvalue of its reduced state at the receiver's side.*

Proof: An $(N + 1)$ -qubit (pure or mixed) state, $\rho_{S_1 S_2 \dots S_N R}$, is multipartite dense codeable with N senders, S_1, S_2, \dots, S_N , and a single receiver, R , if and only if the von Neumann entropy of the reduced state at the receiver's side is greater than that of the state $\rho_{S_1 S_2 \dots S_N R}$, i.e.,

$$S(\rho_R) > S(\rho_{S_1 S_2 \dots S_N R}). \quad (26)$$

Let the eigenvalues, in descending order, of the state ρ_R , be given by $\lambda_R = \{\lambda^1 \geq \frac{1}{2}, 1 - \lambda^1\}$. Let the eigenvalues of the state $\rho_{S_1 S_2 \dots S_N R}$ be $\lambda_{S_1 S_2 \dots S_N R} = \{\mu^i\}_{i=1}^r$, where r is the rank of the matrix, and where the μ^i 's are arranged in descending order. Specifically, μ^1 gives the largest eigenvalue of $\rho_{S_1 S_2 \dots S_N R}$. Now, the ordering between the highest eigenvalues of ρ_R and $\rho_{S_1 S_2 \dots S_N R}$, i.e., between λ^1 and μ^1 , can have three possibilities, i.e., $\lambda^1 > \mu^1$, or they are equal, or $\lambda^1 < \mu^1$.

Let us assume that $\lambda^1 \geq \mu^1$. Then, invoking the condition of majorization [46], we have

$$\lambda_R \succ \lambda_{S_1 S_2 \dots S_N R},$$

which implies

$$S(\rho_R) \leq S(\rho_{S_1 S_2 \dots S_N R}). \quad (27)$$

It immediately implies that the state is not dense codeable. Therefore, to obtain dense codeability of $\rho_{S_1 S_2 \dots S_N R}$, we must have $\lambda^1 < \mu^1$. Hence the proof. ■

Although the above proposition has been presented for qubit systems, it is also valid for an arbitrary (pure or mixed) $(N + 1)$ -party quantum state in arbitrary dimensions, provided ρ_R is of rank 2.

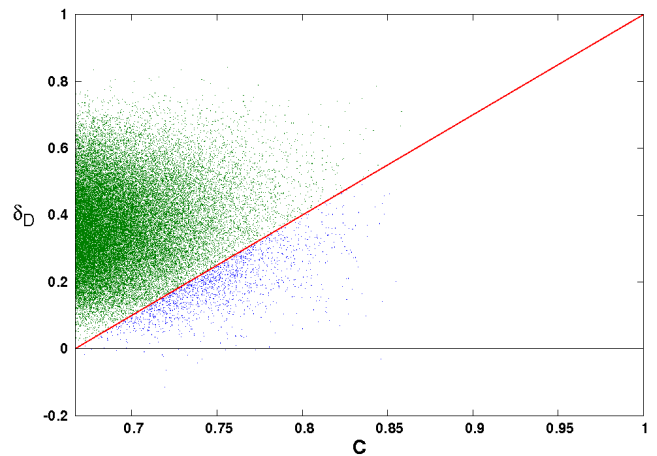


FIG. 4. (Color online.) Discord monogamy score vs. multipartite DC capacity for Haar uniformly generated rank-2 three-qubit states. The red line represents the g GHZ states. About 1.85% of the randomly generated states lie below the red line, and are represented by blue dots. The remaining, represented by green dots, lie above the red line. The horizontal axis is dimensionless while the vertical one is measured in bits.

Let us now move to mixed states with higher-rank. Numerically, to obtain high-rank three-qubit mixed states, one possibility is to generate pure states with more than three parties. For example, to obtain arbitrary rank-4 states of three qubits, 5-qubit pure states can be created randomly, and then two parties traced out. However, numerical searches become inefficient with the increase of number of parties [47]. To overcome this problem, we create mixed states, ρ_8 , of full rank, given by

$$\rho_8 = (1 - p)\rho + \frac{p}{8}I_8, \quad (28)$$

by choosing ρ as arbitrary rank-2 three qubit states, generated randomly from the three-qubit pure states, and where I_8 is the identity matrix on the three-qubit Hilbert space. Moreover, we consider those set of states, ρ , which are dense codeable. In that case, we find that its DC capacity remains nonclassical only for very small values of the mixing parameter p . In Fig. 5, we specifically consider the full rank state, ρ_8 , with ρ given by

$$\rho = q|GHZ\rangle\langle GHZ| + (1 - q)|GHZ'\rangle\langle GHZ'|, \quad (29)$$

where $|GHZ'\rangle = \frac{1}{\sqrt{2}}(|000\rangle - |111\rangle)$. We now plot, in Fig. 5, the discord monogamy score and the raw DC capacity with respect to the mixing parameter p . For $q = 1$ or $q = 0$, and $p = 0$, the capacity is maximum and δ_D also gives a maximum. Fig. 5 shows that there is a small region in which the state remains dense codeable, only when δ_D is very high. It is plausible that the capacity of dense coding for mixed states decreases with the increase of rank of the state. This is intuitively understandable from the condition in Proposition 1, since

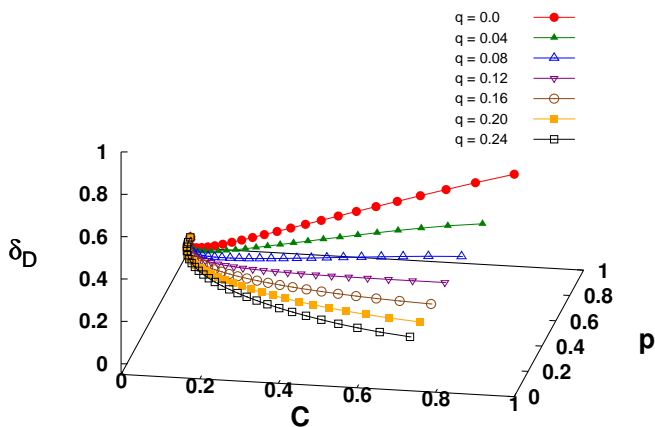


FIG. 5. (Color online.) Discord monogamy score and the raw DC capacity are plotted against the mixing parameter p , for the rank-8 state, $\rho_8 = (1-p)\rho + \frac{p}{8}I$. Here $\rho = q|GHZ\rangle\langle GHZ| + (1-q)|GHZ'\rangle\langle GHZ'|$. Each value of q provides a curve, and we present several exemplary curves in the figure. All the quantities plotted are dimensionless, except δ_D , which is measured in bits.

the typical high-rank state can have eigenvalues more distributed than the typical low-rank state. Therefore, the maximal eigenvalue of a shared state typically gives a lower value than that of the receiver's side, and the condition in Proposition 1 is thereby satisfied for a very small set of states.

V. RELATION BETWEEN CAPACITY OF DENSE CODING AND QUANTUM CORRELATIONS FOR NOISY CHANNELS

In this section, we consider the DC capacity of the noisy channels, for both correlated and uncorrelated noise, for the $(N+1)$ -party state, $\rho_{S_1 S_2 \dots S_N R}$, shared between N senders and a single receiver. Here we assume that the N senders individually apply local unitary operations on their parts of the shared state and send their encoded parts through a covariant noisy channel (see Sec. III B). We now address the extent to which the relation, established in Sec. IV, between multiparty DC capacity for the noiseless channel and multipartite quantum correlation measures, in the case of pure shared quantum states, still remains valid for the noisy channel scenario. To this end, we consider two extreme scenarios, one in which the noise between the different sender qubits are fully correlated, and another in which the same are uncorrelated.

A. Fully correlated Pauli channel

An $(N+1)$ -qubit state, $\rho_{S_1 S_2 \dots S_N R}$, after being acted on by the fully correlated Pauli channel, is given by

$$\Lambda^P(\rho_{S_1 S_2 \dots S_N R}) = \sum_{i=0}^3 q_m (\sigma_{S_1}^m \otimes \dots \otimes \sigma_{S_N}^m \otimes I_R) \rho_{S_1 S_2 \dots S_N R} (\sigma_{S_1}^m \otimes \dots \otimes \sigma_{S_N}^m \otimes I_R), \quad (30)$$

where $\sum_{m=0}^3 q_m = 1$, and $q_m \geq 0$, and where we denote, for simplicity, $\sigma_x = \sigma^1, \sigma_y = \sigma^2, \sigma_z = \sigma^3$, and the identity matrix as σ^0 for the sender qubits. The receiver qubit is acted on only by the identity operator, which we denote by I_R .

We now establish the parallel of the ordering in Theorem 1 for the fully correlated Pauli channel.

Theorem 3: *If the multiparty dense coding capacity of an arbitrary three-qubit pure state, $|\psi\rangle$, is the same as that of the $gGHZ$ state in the presence of the fully correlated Pauli channel, then the genuine multipartite entanglement, GGM, of that arbitrary pure state is bounded below by that of the $gGHZ$ state, i.e.,*

$$\mathcal{E}(|\psi\rangle) \geq \mathcal{E}(|gGHZ\rangle), \quad (31)$$

provided the following two conditions hold: (i) the largest eigenvalue of the noisy $|\psi\rangle$ state is bounded above by $\max\{q_1 + q_2, 1 - q_1 - q_2\}$, and (ii) the receiver's side gives the maximum eigenvalue for the GGM of $|\psi\rangle$.

Proof: The capacities of multiparty dense coding of the $gGHZ$ state and the three-qubit pure state, $|\psi\rangle$, after being acted on by the correlated noisy channel, can be obtained from Eq. (15), and are given respectively by

$$C_c^{noisy}(|gGHZ\rangle) = \frac{2}{3} + \frac{H(\alpha) - S(\tilde{\rho}_{gGHZ})}{3} \quad (32)$$

and

$$C_c^{noisy}(|\psi\rangle) = \frac{2}{3} + \frac{H(\lambda_R) - S(\tilde{\rho}_\psi)}{3} \quad (33)$$

where $\tilde{\rho}_{gGHZ} = \Lambda^P((U_{S_1 S_2}^{min} \otimes I_R)|gGHZ\rangle\langle gGHZ| (U_{S_1 S_2}^{min\dagger} \otimes I_R))$ with $U_{S_1 S_2}^{min}$ being the unitary operator at the senders' part that minimizes the relevant von Neumann entropy (see Sec. III B). Here, we are considering only those cases for which the (noisy) capacities of both the $gGHZ$ state as well as of the $|\psi\rangle$ are non-classical, i.e., the corresponding noisy states are dense codeable. Replacing $|gGHZ\rangle$ by $|\psi\rangle$ in $\tilde{\rho}_{gGHZ}$, one obtains $\tilde{\rho}_\psi$. The $U_{S_1 S_2}^{min}$ is of course a function of the input state. Here, $\lambda_R \geq \frac{1}{2}$ denotes the maximum eigenvalue of the reduced density matrix ρ_R of $|\psi\rangle$. For $0 \leq x \leq 1$, $H(x)$ denotes the binary entropy function $-x \log_2 x - (1-x) \log_2 (1-x)$. For the $gGHZ$ state, the von Neumann entropy of the resulting state after sending through the fully correlated Pauli channel is $S(\tilde{\rho}_{gGHZ}) = H(q_1 + q_2)$, which is independent of the choice of the local unitary operators.

Equating Eqs. (32) and (33), we have,

$$\begin{aligned} H(\alpha) &= H(\lambda_R) + [H(q_1 + q_2) - S(\tilde{\rho}_\psi)] \\ &= H(\lambda_R) + [H(q_1 + q_2) - H(\{\lambda_i\})], \end{aligned} \quad (34)$$

where $\{\lambda_i\}_{i=1}^8$ are the eigenvalues of $\tilde{\rho}_\psi$ in descending order. Here $H(\{\lambda_i\}) = -\sum_i \lambda_i \log_2 \lambda_i$. If we assume that $\lambda_1 \leq \max\{q_1 + q_2, 1 - q_1 - q_2\}$, we have $\{\lambda_i\} \prec \{q_1 + q_2, 1 - q_1 - q_2\}$. The relation between majorization and Shannon entropy [46] then implies that $H(q_1 + q_2) \leq H(\{\lambda_i\})$. Therefore, from Eq. (34), we have

$$H(\alpha) \leq H(\lambda_R) \Rightarrow \alpha \geq \lambda_R, \quad (35)$$

where we assume $\alpha \geq \frac{1}{2}$.

The GGM for the g GHZ state and the three-qubit state, $|\psi\rangle$, are respectively given by $\mathcal{E}(|gGHZ\rangle) = 1 - \alpha$ and $\mathcal{E}(|\psi\rangle) = 1 - \lambda_{max}$, where λ_{max} is the maximum eigenvalue among the eigenvalues of all the local density matrices of $|\psi\rangle$. If we assume that the eigenvalue from the receiver's side attains the maximum, i.e., if $\lambda_R = \lambda_{max}$, using Eq. (35), we obtain

$$\mathcal{E}(|gGHZ\rangle) = 1 - \alpha \leq 1 - \lambda_R = \mathcal{E}(|\psi\rangle). \quad (36)$$

Hence the proof. \blacksquare

The above theorem ekes out a subset of the pure three-qubit state space, for which the g GHZ state is more robust with respect to multiparty DC capacity, against fully correlated Pauli noise, as compared to any member of the said subset, provided the g GHZ and the said member have equal multiparty entanglement, as quantified by their GGMs. This specific subset of states are those which satisfy both the conditions (i) and (ii). The situation, at least for this specific subset, has therefore exactly reversed with respect to the noiseless scenario, as enunciated in Theorem 1. For a given amount of multiparty entanglement content, as quantified by the GGM, the g GHZ state can now be better than other pure states, with respect to the multiparty classical capacity. The noisy quantum channel can therefore reverse the relative capabilities of classical information transfer of different states in multiparty quantum systems. The result is much more general than what is contained in Theorem 3. First of all, the result in Theorem 3 holds even if we replace the GGM as the multiparty quantum correlation measure by the tangle or the discord monogamy score, provided we consider the set of three-qubit pure states for which the two-party concurrences or quantum discords respectively vanish, and the receiver is used as the nodal observer. Comparing now with Theorem 2, we see that the phenomenon of the inversion of the relative capabilities for classical information transfer is generic in this sense: it applies irrespective of whether the GGM, or the tangle, or the discord monogamy score is used to measure the multiparty quantum correlation content. Secondly, we will show below that the phenomenon of reversal of information carrying capacity with the addition of noise actually holds for a much larger class of states than the ones covered by the conditions (i) and (ii) in Theorem 3. We resort to numerical searches by generating Haar uniform three-qubit pure states for this purpose. The following picture is therefore emerging. Given a three-qubit pure state, $|\psi\rangle$, and a g GHZ state with the same multiparty quantum correlation content, the multiparty

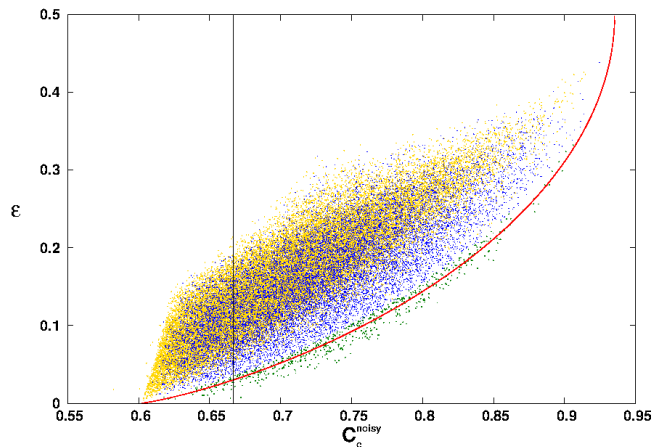


FIG. 6. (Color.) GGM (vertical axis) vs. the raw DC capacity (horizontal axis) under the fully correlated Pauli channel, when the shared state is an arbitrary three-qubit pure state (orange, green, and blue dots) or the g GHZ state (red line). For all the states, the noise in the channel is fixed to 0.19. We choose $q_0 = q_3 = 0.485$, and $q_1 = q_2 = 0.015$ as noise parameters for the arbitrary as well as the g GHZ state. This corresponds to the Case 1 of Sec. V A. See the discussion there for further details. Both the axes are dimensionless. The vertical line at the $C_c^{\text{noisy}} = 2/3$ helps to readily read out the actual capacity from the raw capacity.

DC capacity of the g GHZ state is much less affected by noise than a large class of $|\psi\rangle$, and in many cases, the ordering of the capacities can get reversed in the noisy case as compared to the order in the noiseless case.

To perform the numerical searches, we first observe that the $C_c^{\text{noisy}}(|gGHZ\rangle)$ depends on the sum of the two parameters q_1 and q_2 (or $q_0 + q_3$). By fixing $q_1 + q_2 = c$ (or $q_0 + q_3 = 1 - c$), one can set the noise parameter for the g GHZ state. However, the situation for an arbitrary state, $|\psi\rangle$, is more involved, for which the capacity of dense coding, $C_c^{\text{noisy}}(|\psi\rangle)$, depends individually on all the $\{q_i\}$. To quantify the randomness of $\{q_i\}$, and indeed the noise in the channel, we consider the Shannon entropy, $H(\{q_i\})$. We now consider two extreme cases: one for which $H(\{q_i\})$ is maximum and the other in which the same is a minimum, both subject to the constraint $q_1 + q_2 = c$, where $0 \leq c \leq 1$. The maximum of $H(\{q_i\})$ is attained when $q_1 = q_2 = c/2$ and $q_0 = q_3 = (1 - c)/2$, while the minimum is obtained when any one of the q_1 and q_2 and any one of q_0 and q_3 are zero. It is also evident from Eq. (32), that one should deal with a very low or very high values of c , for the state to remain dense codeable.

We now randomly generate 5×10^4 three-qubit pure states with a uniform Haar measure over that space, and investigate the two extreme cases mentioned above, for fixed $H(q_1 + q_2) = 0.19$. We choose the two sets of values for the q_i 's as follows – Case 1: $q_0 = q_3 = 0.485$, and $q_1 = q_2 = 0.015$ (see Fig. 6), and Case 2: $q_0 = 0.93$, $q_1 = 0.01$, $q_2 = 0.02$, $q_3 = 0.04$ (see Fig. 7). For

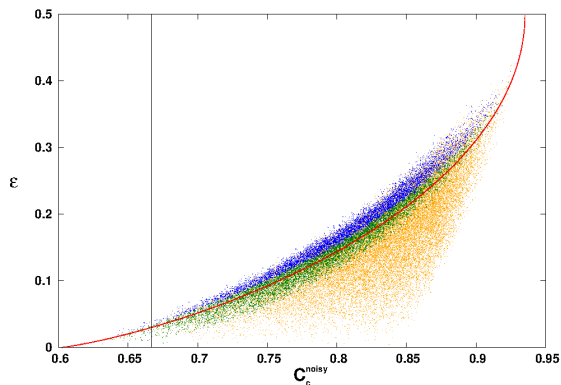


FIG. 7. (Color.) GGM (vertical axis) vs. DC capacity (horizontal axis) under the fully correlated Pauli channel. In this case, we choose $\{q_i\}$ as $q_0 = 0.93, q_1 = 0.01, q_2 = 0.02, q_3 = 0.04$. This corresponds to the Case 2 of Sec. V A. We randomly (Haar uniformly) generate 5×10^4 three-qubit pure states. See text for further details. Both axes represent dimensionless quantities. The vertical line at $C_c^{\text{noisy}} = 2/3$ has the same function as in Fig. 6.

fixed $H(q_1 + q_2) = 0.19$, Case 1 is an example for high noise, and corresponds to the case when $H(\{q_i\})$ is a maximum subject to the constraint $H(q_1 + q_2) = 0.19$, which is the same as the constraint $q_1 + q_2 = 0.03$. Case 2 is an example of low noise, and corresponds to a situation that is close to the case when $H(\{q_i\})$ is a minimum subject to the constraint $H(q_1 + q_2) = 0.19$. We present the low noise case, when the configuration is slightly away from the analytical minimum to provide a more non-trivial example.

Case 1 (Fig. 6): In presence of high noise, we observe that almost all the randomly generated states have shifted to above the g GHZ state (red line) in the plane of GGM and the raw capacity, C_c^{noisy} . As expected, one-third of the randomly generated states satisfy condition (ii) of Theorem 3. A significantly large fraction (98.6%) of them further satisfies condition (i). They are represented by blue dots in Fig. 6 and lie above the g GHZ line. The remaining 1.4% are represented by green dots, and may lie below or above the g GHZ curve. The further states are represented by orange dots. Note that we have plotted the raw capacity in Fig. 6.

Case 2 (Fig. 7): For low noise, the randomly generated states may fall below or above the red line of the g GHZ states. Again, one-third of the generated states satisfy condition (ii). 45.6% of them satisfy condition (i), are represented by blue dots, and fall above the red line. The remaining 54.4% of them are represented by green dots, and can be below or above the g GHZ line. The other two-thirds are represented by orange dots, and can again be either below or above the g GHZ line.

The occurrence of the randomly generated states both below and above the curve for the g GHZ states on the plane of the GGM and the capacity is expected from continuity arguments, for low noise. However, if one makes a

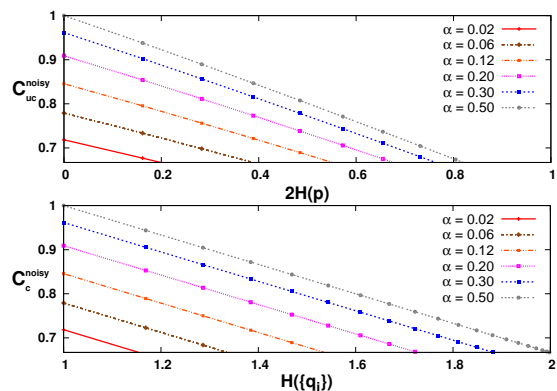


FIG. 8. (Color online.) DC capacity vs. noise for various choices of α in the g GHZ state. In the top panel, the capacity of DC is plotted against the noise of the depolarizing channel, while in the bottom one, the DC capacity is plotted with respect to the noise in the fully correlated Pauli channel, for the g GHZ state. Different curves correspond to different values of α . The vertical axis starts from $2/3$, below which the states are not dense codeable. The states remain dense codeable in the presence of moderate to high Pauli noise while this is not the case for the uncorrelated depolarizing channel. The horizontal axes are measured in bits. All other quantities are dimensionless.

comparison between Figs. 2 and 6, it is revealed that arbitrary three-qubit pure states require higher amount of multipartite entanglement than the g GHZ states to keep themselves dense codeable in the presence of moderate noise.

We have also numerically analyzed the randomly generated states by replacing the GGM with the tangle and with the discord monogamy score. We find the behavior of the DC capacity with these multipartite quantum correlation measures to be similar to that between the DC capacity and the GGM. However, the GGM is more sensitive to noise than tangle or discord monogamy score, in the sense that in the presence of small values of noise parameters, the percentages of states which are below the g GHZ state is much higher in the case of the monogamy score measures than for the GGM.

Therefore, Theorem 3 and the numerical simulations strongly suggest that in the presence of fully correlated Pauli noise, the ratio of multipartite entanglement to the DC capacity of the g GHZ state increases at a slower rate than that of the arbitrary three-qubit pure states, irrespective of the choice of the multipartite quantum correlation measure.

B. Uncorrelated Pauli channel

Consider now a Pauli channel in which the unitary operators acting on different subsystems are not correlated to each other. More specifically, we suppose that each qubit is acted on by a depolarizing channel with noise parameter p . Before analyzing the relation between the

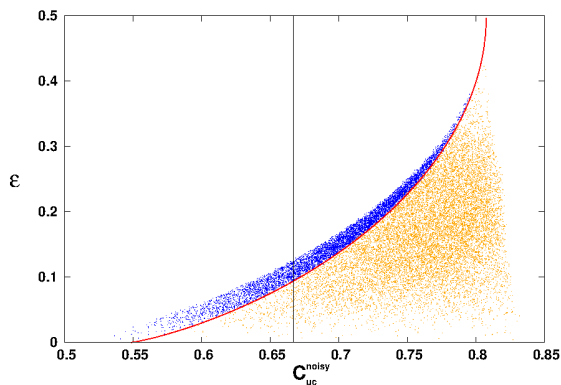


FIG. 9. (Color.) GGM vs. the raw DC capacity, C_{uc}^{noisy} , in the presence of the uncorrelated noise. See text for further details. Both axes represent dimensionless quantities. The vertical line at $C_{uc}^{noisy} = 2/3$ again helps to read the actual capacity from the raw capacity.

multiparty DC capacity and quantum correlation measures, we compare the multiparty dense coding capacities for the correlated channels with those of the uncorrelated ones. A three-qubit state, $\rho_{S_1 S_2 R}$, after the post-encoded qubits pass through independent (uncorrelated) depolarizing channels, of equal strength, p , takes the form

$$\begin{aligned} \mathcal{D}(\rho_{S_1 S_2 R}) &= (1-p)^2 \rho_{S_1 S_2 R} \\ &+ \frac{(1-p)p}{3} \sum_{i=1}^3 (I_{S_1} \otimes \sigma_{S_2}^i \otimes I_R) \rho_{S_1 S_2 R} (I_{S_1} \otimes \sigma_{S_2}^i \otimes I_R) \\ &+ \frac{(1-p)p}{3} \sum_{i=1}^3 (\sigma_{S_1}^i \otimes I_{S_2} \otimes I_R) \rho_{S_1 S_2 R} (\sigma_{S_1}^i \otimes I_{S_2} \otimes I_R) \\ &+ \frac{p^2}{9} \sum_{i,j=1}^3 (\sigma_{S_1}^i \otimes \sigma_{S_2}^j \otimes I_R) \rho_{S_1 S_2 R} (\sigma_{S_1}^i \otimes \sigma_{S_2}^j \otimes I_R). \end{aligned}$$

In the top panel of Fig. 8, the capacity of DC is plotted against the total noise, $2H(p)$, of the uncorrelated channel, for various choices of α in the g GHZ state. The bottom panel represents the DC capacity in the case of the fully correlated Pauli channel with respect to the noise, $H(\{q_i\})$, in this case, for the same g GHZ states. The amount of correlated Pauli noise that can keep the g GHZ state dense codeable, is therefore higher than that of the uncorrelated noise.

To analyze the relation between the DC capacity and quantum correlation, we plot, in Fig. 9, the GGM against C_{uc}^{noisy} , the DC capacity for two senders and a single receiver, with the post-encoded quantum systems being sent to the receiver via uncorrelated depolarizing chan-

nels, for arbitrary pure three-qubit states, which are numerically generated by choosing 5×10^4 random states. We choose the noise parameter, p , as 0.04 for the purpose of the figure (Fig. 9). Fig. 8 shows that for small values of p , the g GHZ state remains dense codeable even for small values of α . In Fig. 9, The blue dots are the ones which satisfy condition (ii) of Theorem 3. Note that condition (i) is not well-defined in the current (uncorrelated) scenario. Most of them lie above the red curve of the g GHZ states. The remaining states are represented by orange dots.

VI. CONCLUSION

For transmission of classical information over noiseless and memory-less quantum channels, the capacity in the case of a single sender and a single receiver is well-studied. However, point-to-point communication is of limited commercial use and the exploration of quantum networks with multiple senders and receivers is therefore of far greater interest. Moreover, creation of multipartite systems with quantum coherence, the essential ingredient for several quantum communication as well as computational tasks, is currently being actively pursued in laboratories around the globe. Establishment of connections between multipartite quantum correlation and capacities are usually hindered by the unavailability of a unique multipartite quantum correlation measure even for pure states, and the plethora of possibilities for multipartite communication protocols.

For a communication scenario involving several senders and a single receiver, we establish the relation between capacities of classical information transmission and multipartite computable quantum correlation measures, both for the noiseless as well as noisy channels. We show that there are hierarchies among multipartite states according to the capacities of the dense coding protocol and hence obtain a tool to classify quantum states according to their usefulness in quantum dense coding. The results can be an important step forward in building up communication networks using multipartite quantum correlated states in realizable systems.

ACKNOWLEDGMENTS

RP acknowledges an INSPIRE-faculty position at the Harish-Chandra Research Institute (HRI) from the Department of Science and Technology, Government of India. We acknowledge computations performed at the cluster computing facility at HRI.

-
- [1] R. Horodecki, P. Horodecki, M. Horodecki, and K. Horodecki, Rev. Mod. Phys. **81**, 865 (2009).
 [2] K. Modi, A. Brodutch, H. Cable, T. Patrek, and V. Ve-

- dral, Rev. Mod. Phys. **84**, 1655 (2012).
 [3] M. Lewenstein, A. Sanpera, V. Ahufinger, B. Damski, A. Sen(De), and U. Sen, Adv. Phys. **56**, 243 (2006).

- [4] L. Amico, R. Fazio, A. Osterloh, and V. Vedral, *Rev. Mod. Phys.* **80**, 517 (2008).
- [5] C.H. Bennett and S.J. Wiesner, *Phys. Rev. Lett.* **69**, 2881 (1992).
- [6] C. H. Bennett, G. Brassard, C. Crépeau, R. Jozsa, A. Peres, and W. K. Wootters, *Phys. Rev. Lett.* **70**, 1895 (1993).
- [7] N. Gisin, G. Ribordy, W. Tittel, and H. Zbinden, *Rev. Mod. Phys.* **74**, 145 (2002).
- [8] H.J. Briegel, D. Browne, W. Dür, R. Raussendorf, and M. van den Nest, *Nat. Phys.* **5**, 19 (2009).
- [9] W.-B. Gao, C.-Y. Lu, X.-C. Yao, P. Xu, O. Gühne, A. Goebel, Y.-A. Chen, C.-Z. Peng, Z.-B. Chen, and J.-W. Pan, *Nat. Phys.* **6**, 331 (2010).
- [10] T. Monz, P. Schindler, J.T. Barreiro, M. Chwalla, D. Nigg, W.A. Coish, M. Harlander, W. Hänsel, M. Hennrich, and R. Blatt, *Phys. Rev. Lett.* **106**, 130506 (2011).
- [11] J.T. Barreiro, J.-D. Bancal, P. Schindler, D. Nigg, M. Hennrich, T. Monz, N. Gisin and R. Blatt, *Nat. Phys.* **9**, 559 (2013).
- [12] C. Negrevergne, T.S. Mahesh, C.A. Ryan, M. Ditty, F. Cyr-Racine, W. Power, N. Boulant, T. Havel, D.G. Cory, and R. Laflamme, *Phys. Rev. Lett.* **96**, 170501 (2006).
- [13] O. Mandel, M. Greiner, A. Widera, T. Rom, T.W. Hänsch, and I. Bloch, *Nature* **425**, 937 (2003).
- [14] M. Cramer, A. Bernard, N. Fabbri, L. Fallani, C. Fort, S. Rosi, F. Caruso, M. Inguscio, and M.B. Plenio, *Nat. Comm.* **4**, 2161 (2013).
- [15] M. Żukowski, A. Zeilinger, M.A. Horne, and H. Weinfurter, *Acta Phys. Pol.* **93**, 187 (1998); M. Hillery, V. Bužek, and A. Berthiaume, *Phys. Rev. A* **59**, 1829 (1999).
- [16] R. Cleve, D. Gottesman, H.-K. Lo, *Phys. Rev. Lett.* **83**, 648 (1999); A. Karlsson, M. Koashi, and N. Imoto, *Phys. Rev. A* **59**, 162 (1999); K. Chen and H.-K. Lo, *Quant. Inf. Comput.* **7**, 689 (2007).
- [17] D. Bruß, D.P. DiVincenzo, A. Ekert, C.A. Fuchs, C. Macchiavello, and J.A. Smolin, *Phys. Rev. A* **57**, 2368 (1998); M. Muraio, D. Jonathan, M. B. Plenio, and V. Vedral, *ibid.* **59**, 156 (1999).
- [18] J. Eisert, T. Felbinger, P. Papadopoulos, M.B. Plenio, and M. Wilkens, *Phys. Rev. Lett.* **84**, 1611 (2000).
- [19] M. Fitz, N. Gisin, and U. Maurer, *Phys. Rev. Lett.* **87**, 217901 (2001).
- [20] P. Badziąg, M. Horodecki, A. Sen(De), and U. Sen, *Phys. Rev. Lett.* **91**, 117901 (2003).
- [21] D. Bruß, G.M. D'Ariano, M. Lewenstein, C. Macchiavello, A. Sen(De), and U. Sen, *Phys. Rev. Lett.* **93**, 210501 (2004).
- [22] M. Demianowicz and P. Horodecki, *Phys. Rev. A* **74**, 042336 (2006).
- [23] L. Czekaj and P. Horodecki, *Phys. Rev. Lett.* **102**, 110505 (2009).
- [24] A. Sen(De) and U. Sen, *Phys. Rev. A* **81**, 012308 (2010).
- [25] W. Dür, G. Vidal, and J.I. Cirac, *Phys. Rev. A*, **62** 062314 (2000).
- [26] D.M. Greenberger, M.A. Horne, and A. Zeilinger, in *Bells Theorem, Quantum Theory, and Conceptions of the Universe*, ed. M. Kafatos (Kluwer Academic, Dordrecht, The Netherlands, 1989).
- [27] A. Sen(De) and U. Sen, arXiv:1002.1253 [quant-ph].
- [28] A. Shimony, *Ann. N.Y. Acad. Sci.* **755**, 675 (1995); H. Barnum and N. Linden, *J. Phys. A* **34**, 6787 (2001); D.A. Meyer and N.R. Wallach, *J. Math. Phys.* **43**, 4273 (2002); T.-C. Wei and P.M. Goldbart, *Phys. Rev. A* **68**, 042307 (2003); M. Balsone, F. Dell'Anno, S. De Siena and F. Illuminati, *Phys. Rev. A* **77**, 062304 (2008).
- [29] V. Coffman, J. Kundu, and W.K. Wootters, *Phys. Rev. A* **61**, 052306 (2000).
- [30] R. Prabhu, A.K. Pati, A. Sen(De), and U. Sen, *Phys. Rev. A* **85**, 040102(R) (2012).
- [31] M.N. Bera, R. Prabhu, A. Sen(De), and U. Sen, *Phys. Rev. A* **86**, 012319 (2012).
- [32] C.H. Bennett, D.P. DiVincenzo, J.A. Smolin, and W.K. Wootters, *Phys. Rev. A* **54**, 3824 (1996); E.M. Rains, *ibid.* **60**, 173 (1999); *ibid.* **60**, 179 (1999); P.M. Hayden, M. Horodecki, and B.M. Terhal, *J. Phys. A: Math. Gen.* **34**, 6891 (2001).
- [33] S. Hill and W.K. Wootters, *Phys. Rev. Lett.* **78**, 5022 (1997); W.K. Wootters, *ibid.* **80**, 2245 (1998).
- [34] G. Vidal and R.F. Werner, *Phys. Rev. A* **65**, 032314 (2002).
- [35] L. Henderson and V. Vedral, *J. Phys. A* **34**, 6899 (2001); H. Ollivier and W.H. Zurek, *Phys. Rev. Lett.* **88**, 017901 (2001).
- [36] J. Oppenheim, M. Horodecki, P. Horodecki, and R. Horodecki, *Phys. Rev. Lett.* **89**, 180402 (2002); M. Horodecki, K. Horodecki, P. Horodecki, R. Horodecki, J. Oppenheim, A. Sen(De), and U. Sen, *ibid.* **90**, 100402 (2003); I. Devetak, *Phys. Rev. A* **71**, 062303 (2005); M. Horodecki, P. Horodecki, R. Horodecki, J. Oppenheim, A. Sen(De), U. Sen, and B. Synak-Radtke, *ibid.* **71**, 062307 (2005).
- [37] B. Groisman, S. Popescu, and A. Winter, *Phys. Rev. A* **72**, 032317 (2005).
- [38] N.J. Cerf and C. Adami, *Phys. Rev. Lett.* **79**, 5194 (1997).
- [39] T.J. Osborne and F. Verstraete, *Phys. Rev. Lett.* **96**, 220503 (2006).
- [40] S. Bose, M.B. Plenio, and V. Vedral, *J. Mod. Opt.* **47**, 291 (2000); T. Hiroshima, *J. Phys. A: Math. Gen.* **34**, 6907 (2001); G. Bowen, *Phys. Rev. A* **63**, 022302 (2001); M. Horodecki, P. Horodecki, R. Horodecki, D. Leung, and B. Terhal, *Quantum Information and Computation* **1**, 70 (2001); X.S. Liu, G.L. Long, D.M. Tong, and F. Li, *Phys. Rev. A* **65**, 022304 (2002); M. Ziman and V. Bužek, *ibid.* **67**, 042321 (2003).
- [41] D. Bruß, M. Lewenstein, A. Sen(De), U. Sen, G.M. D'Ariano, and C. Macchiavello, *Int. J. Quant. Inf.* **4**, 415 (2006).
- [42] M.R. Beran and S.M. Cohen, *Phys. Rev. A* **78**, 062337 (2008); M. Horodecki and M. Piani, *J. Phys. A: Math. Theor.* **45** 105306 (2012).
- [43] Z. Shadman, H. Kampermann, C. Macchiavello, and D. Bruß, *New J. Phys.* **12**, 073042 (2010); *Phys. Rev. A* **84**, 042309 (2011); *Phys. Rev. A* **85**, 052306 (2012); *Quantum Measurements and Quantum Metrology*, **1**, 21 (2013).
- [44] J. Preskill, *Lecture Notes*, available at <http://www.theory.caltech.edu/people/preskill/ph219/>.
- [45] N.D. Mermin, *Phys. Rev. Lett.* **65**, 1838 (1990); M. Ardehali, *Phys. Rev. A* **46**, 5375 (1992); A.V. Belinskii and D.N. Klyshko, *Phys. Usp.* **36**, 653 (1993).
- [46] R. Bhatia, *Matrix Analysis* (Springer-verlag, New York, 1997).
- [47] P. Hayden, D. Leung, P.W. Shor, and A. Winter, *Commun. Math. Phys.* **250**, 371 (2004).